THE JOURNAL OF BIOLOGICAL CHEMISTRY VOL. 289, NO. 15, pp. 10761–10768, April 11, 2014

Hyperactivation of the Human Plasma Membrane Ca^{2+} Pump PMCA h4xb by Mutation of Glu^{99} to Lys*

Received for publication, November 15, 2013, and in revised form, February 11, 2014 Published, JBC Papers in Press, February 28, 2014, DOI 10.1074/jbc.M113.535583

Luciana R. Mazzitelli and Hugo P. Adamo[1]

From the Instituto de Química y Fisicoquímica Biológicas-Departamento de Química Biológica, Facultad de Farmacia y Bioquímica, Universidad de Buenos Aires, Junín 956, 1113 Buenos Aires, Argentina

Background: The calmodulin-stimulated human plasma membrane Ca^{2+} pump is regulated by autoinhibition.
Results: The E99K mutation deregulates the pump increasing its maximal activity at saturating concentrations of Ca^{2+}.
Conclusion: The cytosolic portion of the M1 transmembrane segment is critical for inhibition by the extreme C-terminal autoinhibitory domain.
Significance: This work presents new insights into the structure and the mechanism of human PMCA autoinhibition.

The transport of calcium to the extracellular space carried out by plasma membrane Ca^{2+} pumps (PMCAs) is essential for maintaining low Ca^{2+} concentrations in the cytosol of eukaryotic cells. The activity of PMCAs is controlled by autoinhibition. Autoinhibition is relieved by the binding of Ca^{2+}-calmodulin to the calmodulin-binding autoinhibitory sequence, which in the human PMCA is located in the C-terminal segment and results in a PMCA of high maximal velocity of transport and high affinity for Ca^{2+}. Autoinhibition involves the intramolecular interaction between the autoinhibitory domain and a not well defined region of the molecule near the catalytic site. Here we show that the fusion of GFP to the C terminus of the h4xb PMCA causes partial loss of autoinhibition by specifically increasing the V_{max}. Mutation of residue Glu^{99} to Lys in the cytosolic portion of the M1 transmembrane helix at the other end of the molecule brought the V_{max} of the h4xb PMCA to near that of the calmodulin-activated enzyme without increasing the apparent affinity for Ca^{2+}. Altogether, the results suggest that the autoinhibitory interaction of the extreme C-terminal segment of the h4 PMCA is disturbed by changes of negatively charged residues of the N-terminal region. This would be consistent with a recently proposed model of an autoinhibited form of the plant ACA8 pump, although some differences are noted.

Calcium plays an essential signaling role in cell biology. Because of its electrochemical gradient, Ca^{2+} is continuously entering the cell. The plasma membrane Ca^{2+} pump (PMCA)[2] is one of the two known systems that can be used by animal cells to return Ca^{2+} to the extracellular space (1). The other system is the Na^{+}-Ca^{2+} exchanger present in excitable cells. In humans, the PMCA is coded for by four genes, genes 1–4, and a variety of isoforms generated by alternative mRNA splicing (2). The h4 PMCA is found virtually in all human tissues, and the splice variant *xb* is the most studied isoform. The PMCA is a P-type ATPase belonging to the P2B subgroup, which includes those P-type ATPases that are regulated by autoinhibition (3). The PMCA is mainly activated by calmodulin, whose effects can be mimicked by acidic lipids (4). In the animal PMCA, the calmodulin-binding autoinhibitory region is located at the C terminus of the molecule, whereas in the plant PMCA, it is located at the N terminus of the molecule.

Although the structure of PMCAs at the atomic level is not yet known, computer modeling and sequence comparisons indicate that the overall domain organization of PMCAs closely resembles that of other P-ATPases (5, 6), with a transmembrane region of 10 segments (M1–M10) and three major catalytic domains (the nucleotide-binding (N), the phosphorylation (P), and the actuator (A) domains, exposed to the cytosol). Two amino acid segments, one at the C-terminal region following M10 and the other in the A-M3 linker, are characteristic of animal PMCAs and have regulatory functions. The PMCA protein can exist in two states: the autoinhibited state, in which the autoinhibitory region interacts with another part of the molecule and locks the enzyme in a state of low activity and low Ca^{2+} affinity and the activated or deregulated state, in which binding of Ca^{2+}-calmodulin to the regulatory region changes its interaction with the autoinhibitory receptor site with a consequent increase in the maximal velocity (V_{max}) for Ca^{2+} transport and the apparent affinity for Ca^{2+}. In the h4xb PMCA, the C-terminal regulatory domain has been subdivided into a C domain of about 28 amino acids (residues 1086–1113), which binds calmodulin, and an I domain, which comprises the 44 residues further downstream but is less well defined (7) (Fig. 1). The extreme C-terminal segment has been found to contain a PDZ-binding domain, which allows interaction with other proteins (8). However, studies of C-terminally truncated mutants of h4xb have indicated that the removal of the last 48 amino acids has no apparent consequences for the function of the pump (7). Further removal of up to 92 C-terminal residues, with the consequent deletion of the I domain, produces an enzyme that still

* This work was supported by Grants UBACYT 20020100100800 from Universidad de Buenos Aires, PIP 2022 from Consejo Nacional de Investigaciones Científicas y Técnicas, and Agencia Nacional de Promoción Científica y Tecnológica Prestamo BID 2134.

[1] To whom correspondence should be addressed: IQUIFIB, Facultad de Farmacia y Bioquímica, UBA, Junín 956, 1113 Buenos Aires, Argentina. Tel.: 5411-4-9648289 (ext. 125); Fax: 5411-49625457; E-mail: hpadamo@qb.ffyb.uba.ar.

[2] The abbreviations used are: PMCA, plasma membrane Ca^{2+} pump; $C_{12}E_{10}$, polyoxyethylene 10 lauryl ether; SERCA, sarcoendoplasmic Ca^{2+}-ATPase; CaM, calmodulin; h4xb, plasma membrane Ca^{2+} pump derived from the human gene 4, spliced form *x* at splicing site A and spliced form *b* at splicing site C; CaMBS, calmodulin-binding site.

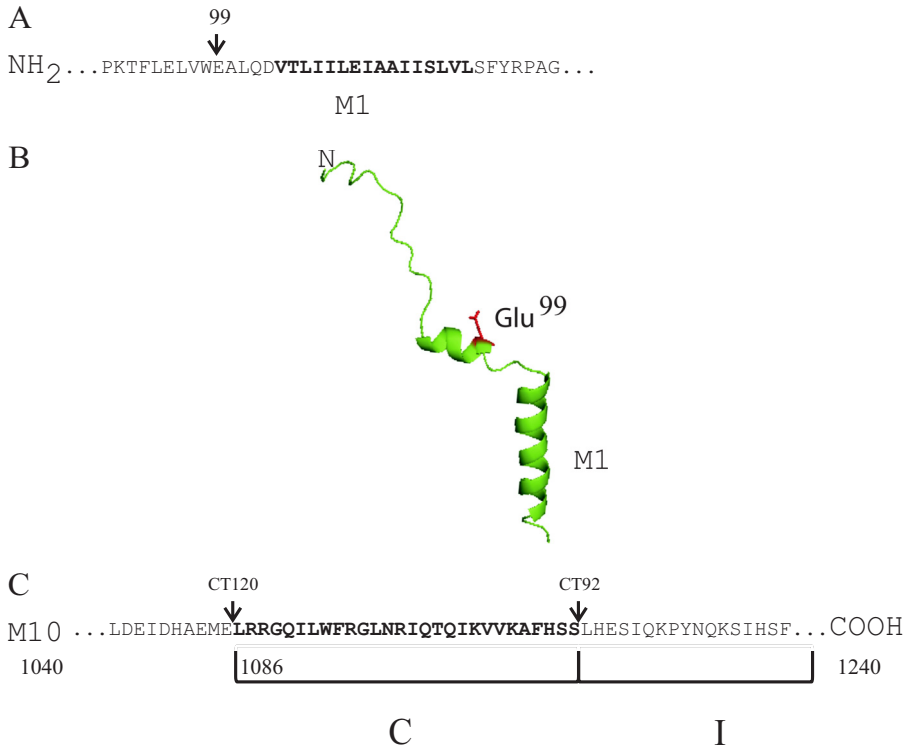

FIGURE 1. *A*, amino acid sequence of the predicted transmembrane helix M1 in the N-terminal region of h4xb PMCA. The portion of M1 predicted to cross the lipid bilayer is shown in boldface type. *B*, homology model of the transmembrane helix M1 of h4xb PMCA. The model was obtained by the Swissprot modeler using SERCA 3w5b as template. *C*, amino acid sequence of the C-terminal segment of the h4xb PMCA. The C terminus of the truncated CT120 and CT92 mutants is marked. The main calmodulin-binding autoinhibitory site or domain C and the accessory inhibitory segment called domain I are indicated.

binds calmodulin and has an affinity for Ca^{2+}, characteristic of the inhibited state, but has a somewhat higher V_{max} (9). Finally, in the CT120 truncated mutant lacking the C and I domains, autoinhibition is totally lost, and the pump attains a V_{max} and a $K_{0.5}$ for Ca^{2+} that are similar to those of the calmodulin-activated enzyme (10).

Recent work has revealed the structure of the N-terminally located autoinhibitory domain of the plant PMCA ACA8 (11). The structure of this PMCA indicates that the calmodulin-bound autoinhibitory domain is a long helix with two calmodulin binding sites, CaMBS1 and CaMBS2, with estimated K_d values for calmodulin of 13 and 500 nM, respectively. Comparison of the N-terminal amino acid sequence of ACA8 with the C-terminal sequence of the human PMCA has revealed that both calmodulin binding sites are conserved in some of the hPMCA splice variants (11).

The site of interaction between the autoinhibitory domains and the catalytic region of PMCAs is still not well defined. Cross-linking experiments using the synthetic peptide C28W made after the sequence of the autoinhibitory domain C of h4xb PMCA have revealed that the N-terminal half of this sequence interacts with the N domain (Cys^{537}–Thr^{544}), whereas the C-terminal part interacts with the A domain (Ile^{206}–Val^{271}) (12, 13). On the other hand, mutations of specific residues in the linker segments connecting the A domain with M1, M2, and M3 have been shown to generate deregulated ACA pumps, indicating that these structures are particularly important for autoinhibition (14). Previous work from our laboratory has indicated that also the N-terminal part of the PMCA molecule is involved in autoinhibition (15). Here we present results indicating that residue Glu^{99} in the acidic cluster at the N-terminal portion of the M1 transmembrane segment and the C-terminal segment of the h4xb PMCA are critical for decreasing the V_{max} in the autoinhibited state.

MATERIALS AND METHODS

Chemicals—Polyoxyethylene 10 lauryl ether ($C_{12}E_{10}$), phosphodiesterase 3′,5′-cyclic nucleotide activator (calmodulin) from bovine brain, calmodulin-agarose, ATP (disodium salt, vanadium-free), sodium dodecyl sulfate (SDS), yeast synthetic drop-out media supplement without leucine, yeast nitrogen base without amino acids, dextrose, and all other chemicals were obtained from Sigma. L-α-Phosphatidylcholine 95% (catalog no. 198662) from chicken egg was obtained from Avanti Polar Lipids, Inc. Tryptone and yeast extract were from Difco. [γ-^{32}P]ATP was provided by PerkinElmer Life Sciences. Salts and reagents were of analytical grade.

Constructs of DNA Coding for Glu^{99} Mutants and C-terminal Deletion (CT92)—The cDNA coding for mutants E99K and E99Q were obtained by a two-step PCR in a standard megaprimer protocol (16) using *Pfu* DNA polymerase and primers His (5′-CTGCAGGTCGACCATGGCGCATCACCATCACCATCACAACCCATCAGACCGTGTCTTGCCTGCCAA-3′, primer 2096 (5′-TGACAACATCAACACAGCCCGGGCCATTGCCACCA-3′ and the following mutagenic primers: E99K, 5′-GCGTGACATCTTGAAGAGCTTTCCACACTAATTCTAAG-3′ and E99Q 5′-GCGTGACATCTTGAAGAGCTTGCCACACTAATTCTAAG-3′. Primer His con-

tains a restriction site for nuclease MluI at its 5′-position that matches a unique site for nuclease MluI introduced at position 4 of the cDNA of h4xb PMCA (15), whereas primer 2096 anneals to h4xb DNA downstream of a naturally occurring BspEI unique site. Primers E99K and E99Q have the same DNA sequence as the h4xb PMCA, except for the nucleotide base corresponding to position 296, where the original guanine (G) nucleotide was replaced by an adenine (A) or cytosine (C), respectively, to achieve a change in the coding sequence of Glu^{99} for lysine or glutamine.

During the first PCR, a fragment was amplified using the h4xb PMCA cDNA as template and primers His and E99K. The 330-bp His-E99K product was isolated by electrophoresis in a 1.5% agarose gel and extracted using DNA Qiaex II (Qiagen). The purified His-E99K fragment was used in the next PCR step along with primer 2096, using the cDNA coding for h4xb PMCA as template. The 2144-bp His-2096 fragment was digested with MluI and BspEI and subcloned into the corresponding position of h4xb PMCA inserted into the SalI-ApaI sites of vector pYX112 (kindly gifted by Dr. Jeffrey Harper). A similar approach was used to obtain the E99Q mutant but using primer E99Q in the first PCR instead. The introduction of the desired mutation to the h4xb PMCA cDNA was confirmed by DNA sequencing.

To obtain the cDNA lacking the final DNA bases coding for the last 92 amino acids of h4xb PMCA (CT92), we used primer A (GCCCATGGCCTGTGATGGACT) and primer CT92 (TACTTTGGGCCCTTAGCATGCGGAACTATGGAACGCTTTGACC) in a single-step PCR protocol. Primer A anneals upstream the naturally occurring BspEI restriction site of the h4xb PMCA cDNA sequence, whereas primer CT92 has a unique site for the restriction endonucleases SphI and ApaI. A fragment of ~1500 bp was amplified using these two primers. The product of this PCR (A-CT92) was isolated by electrophoresis in a 1% agarose gel, extracted using DNA QiaexII (Qiagen), and then used to replace the segment between the BspEI and ApaI sites in the original cDNA of h4xb PMCA cloned into vector pYX112. For the addition of GFP, the cDNA sequence of GFP was digested from vector pMP625 coding for the GFP-Spf1 gene (17) with the restriction endonuclease SphI. The digestion product of ~750 bp was isolated by electrophoresis in a 1.3% agarose gel, extracted using DNA QiaexII, and then cloned into the same digestion site (SphI) of the CT92 construction cloned into vector pYX112. The correct insertion of the GFP gene was checked by sequencing. To obtain the mutants in vector pMP625, the different constructions were digested with the restriction endonucleases SalI and ApaI. The digestion products were isolated in a 1% agarose gel and then subcloned into the polyclonal site of pMP625 between the XhoI and ApaI sites.

Yeast Strain, Transformation, and Growth Media—*Saccharomyces cerevisiae* strain DBY 2062 (MATa his4–619 leu2–3,112) (18) was used for expression and purification. Yeast cells were transformed with vector pMP625 containing a Leu^+ marker and the PMAI promoter. For transformation with the plasmid construct, a lithium acetate/polyethylene glycol method was used (19). The cells were grown in complete medium (0.75% yeast extract, 1.13% tryptone, 2.2% dextrose), and transformants were selected for their ability to grow in the absence of leucine on plates containing 6.7% yeast-nitrogen base without amino acids (YNB), 0.67% complete supplemented medium minus Leu (Leu^-), 2.2% dextrose, and 1.5% agar.

S. cerevisiae strain K616 (MATα pmr1::HIS3 pmc::TRP1 cnb1::LEU2, ura3) (20) was used to express the h4xb and the mutant PMCAs for the complementation assays. The different constructs were cloned into the yeast expression vector pYX112. The transformants were selected for their ability to grow in the absence of uracil on plates containing 6.7% YNB, 0.67% complete supplemented medium minus Ura (Ura^-), 2.2% dextrose, 0.05% MES, pH 6.0, 10 mM Cl_2Ca, and 1.5% agar. For complementation studies, Ura^+ colonies were grown overnight at 28 °C and then transferred into fresh medium. Then 15 μl of log phase culture were streaked onto plates lacking uracil and containing either 10 mM Cl_2Ca or 10 mM EGTA, pH 6.0. The plates were allowed to grow for 72 h at 28 °C.

Membrane Isolation and Purification of PMCA—The wild type h4xb and mutant PMCAs were purified as described previously (15). Briefly, 4 liters of yeast cells expressing the h4xb or mutant proteins were grown in YNB Leu^- medium at 28 °C in glass flasks with agitation, and after the culture reached an approximate $A_{600} = 1.5$, 1 liter of complete medium was added. The incubation continued for 6 h ($A_{600} = 4.0–5.0$). Total yeast membranes were solubilized with $C_{12}E_{10}$, and the PMCA was purified by calmodulin affinity chromatography as described previously (15). About 150 μg of purified PMCA was obtained from one batch of yeast.

Ca^{2+}-ATPase Activity—Ca^{2+}-ATPase activity was estimated from the release of $[^{32}P]P_i$ from [γ-^{32}P]ATP at 37 °C (21) in 0.3 ml of ATPase reaction medium containing 20 mM HEPES-K (pH 6.80 at 37 °C), 100 mM KCl, 4 mM $MgCl_2$, 500 μM EGTA, and enough $CaCl_2$ and calmodulin to give the Ca^{2+} and calmodulin concentrations indicated in each experiment. Prior to the addition to the reaction medium, 1 μg of the enzyme (50 μl) was gently stirred for 5 min with 5 μl of a sonicated mixture of 29 mg/ml phosphatidylcholine and 57 mg/ml $C_{12}E_{10}$. $C_{12}E_{10}$ was partially removed by adding 0.01 g of prewashed wet Bio-Beads SM-2 (Bio-Rad). The mixture was stirred at room temperature for another 25 min, and the Bio-Beads were separated by filtration. The PMCA was incubated for 3 min at 37 °C with the reaction medium before the initiation of the reaction by adding 3 mM [γ-^{32}P]ATP. The reaction was finished by acid denaturation after 30 min. During this period, the amount of P_i released from ATP increased linearly with time. The concentration of free Ca^{2+} in the reaction medium was calculated using the WebmaxC Standard program.

SDS-PAGE and Protein Quantitation—SDS electrophoresis was carried out as described previously (22). Proteins were electrophoresed on a 7.5% acrylamide gel according to Laemmli (23) and revealed by Coomassie Blue staining. The protein concentration was initially estimated by the method of Bradford (24) using bovine serum albumin as a standard. For a more precise quantitation of the PMCA protein in each preparation, the samples were analyzed by SDS-PAGE using bovine serum albumin as a standard, and the intensity of the bands was compared using Gel-Pro Analyzer (MediaCybernetics Inc.) after staining the gels with Coomassie Blue.

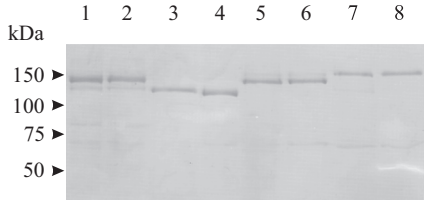

FIGURE 2. **SDS-PAGE of purified h4xb and mutant proteins.** 0.8 μg of the CaM affinity-purified proteins were loaded on each lane of a 7.5% SDS-PAGE and stained with Coomassie Blue. h4xb (*lane 1*), E99K (*lane 2*), CT92 (*lane 3*), E99K-CT92 (*lane 4*), CT92-GFP (*lane 5*), E99K-CT92-GFP (*lane 6*), h4xb-GFP (*lane 7*), and E99K-GFP (*lane 8*).

Data Analysis—Data presented in this work are representative of at least three independent experiments containing a single measurement of the activity at each Ca^{2+} concentration. Equations were fitted to the experimental data using the SigmaPlot 10 scientific data analysis and graphing software (Systat Software Inc.).

RESULTS

Purification of the Wild Type and Mutant h4xb PMCA Proteins—Microsomes obtained from *S. cerevisiae* cells expressing the h4xb PMCA wild type and mutant proteins were solubilized with the detergent $C_{12}E_{10}$ and purified by calmodulin affinity chromatography. Fig. 2 shows the analysis of the purified samples by SDS-PAGE and Coomassie Blue staining. All of the purified proteins exhibited one major band that migrated according to their expected size.

The Fusion of GFP to the C-terminal End of the h4xb PMCA Increased the V_{max}—We have previously reported that the h4xb PMCA containing GFP at its C terminus is still autoinhibited and hence activated by Ca^{2+}-calmodulin (15). A more detailed comparison of the activity of wild type h4xb and h4xb-GFP as a function of Ca^{2+} concentration is presented in Fig. 3. It is clear that, in the absence of calmodulin, the apparent affinity for Ca^{2+} of h4xb-GFP was similar to that of the autoinhibited wild type enzyme. However, at saturating concentrations of Ca^{2+}, the h4xb-GFP enzyme attained a V_{max} 10–20% higher.

The Fusion of GFP to the CT92 Mutant Resulted in a Nearly Fully Active Enzyme—It has been shown previously that the removal of the C-terminal 92 amino acids in the CT92 mutant increases by about 20% the V_{max} in the absence of calmodulin but does not perturb autoinhibition by the C domain, and thus the CT92 enzyme exhibits a low apparent Ca^{2+} affinity (9). Thus, we investigated the effect of the fusion of GFP on the autoinhibition by the C domain by adding GFP at the end of the CT92 mutant. Results in Fig. 4 show that, in the absence of calmodulin, the CT92-GFP mutant exhibited a V_{max} of about 80% and a high apparent affinity for Ca^{2+} similar to that of the calmodulin-activated enzyme.

The E99K Mutation in the A-M1 Linker Increased the V_{max} of the Autoinhibited Enzyme—We have reported previously that the activation of PMCA by the binding of calmodulin at the C-terminal autoinhibitory region of the molecule involves rearrangements at the other end of the molecule (15). Because random mutagenesis of the plant PMCA ACA2 has indicated that the E167K mutation in the cytoplasmic portion of the M1 transmembrane segment is important for autoinhibition (14), we

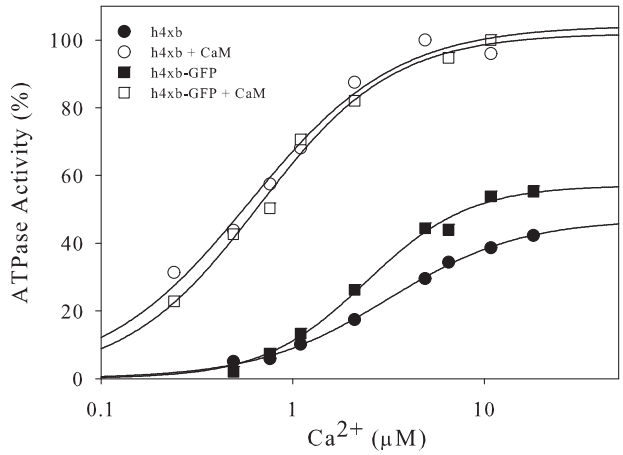

FIGURE 3. **Dependence of Ca^{2+}-ATPase activity of mutant h4xb-GFP and wild type h4xb pumps on Ca^{2+} concentration.** The Ca^{2+}-ATPase activity was assayed at variable free Ca^{2+} concentrations in the absence or presence of 200 nM calmodulin. The activities are expressed relative to the maximum activity of each enzyme measured at saturating Ca^{2+} in the presence of 200 nM calmodulin. The *lines* represent the best fit of the data given by the Hill equation.

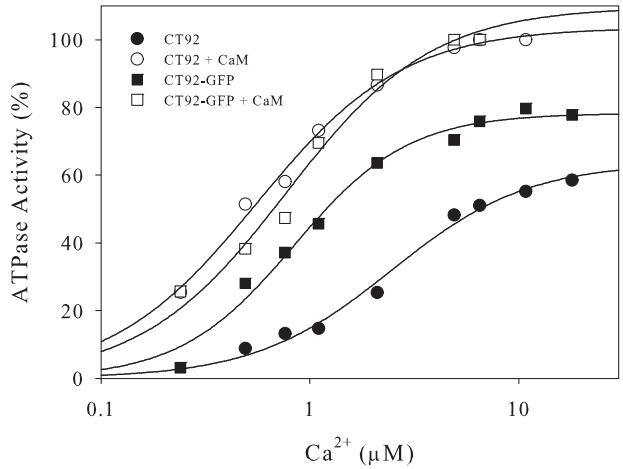

FIGURE 4. **Dependence of Ca^{2+}-ATPase activity of the CT92 and CT92-GFP mutant enzymes on Ca^{2+} concentration.** The Ca^{2+}-ATPase activity was assayed at variable free Ca^{2+} concentrations in the absence or presence of 200 nM calmodulin. The activities are expressed relative to the maximum activity of each enzyme measured at saturating Ca^{2+} in the presence of 200 nM calmodulin. The *lines* represent the best fit of the data given by the Hill equation.

chose to investigate the effects of a similar change in the corresponding residue Glu^{99} of the h4xb PMCA. In the absence of calmodulin, the E99K h4xb mutant showed an apparent affinity for Ca^{2+} characteristic of the autoinhibited enzyme, but its V_{max} was high and almost insensitive to calmodulin, indicating that the mutation had deregulated the h4xb enzyme by increasing its V_{max} (Fig. 5*A*). A mutant of the h4xb PMCA containing the change E99Q was also constructed, and the measurements of the Ca^{2+} dependence of the ATPase activity showed that it had a V_{max} and apparent affinity for Ca^{2+} similar to that of the wild type h4xb (not shown). We further characterized the effect of the E99K mutation by introducing this change in the CT92-truncated h4xb pump. In the absence of calmodulin, the E99K-CT92 mutant had an apparent affinity for Ca^{2+} as low as that of the wild type h4xb PMCA but with a V_{max} higher than that of the CT92 enzyme (Fig. 5*B*). As expected, the C-terminal addi-

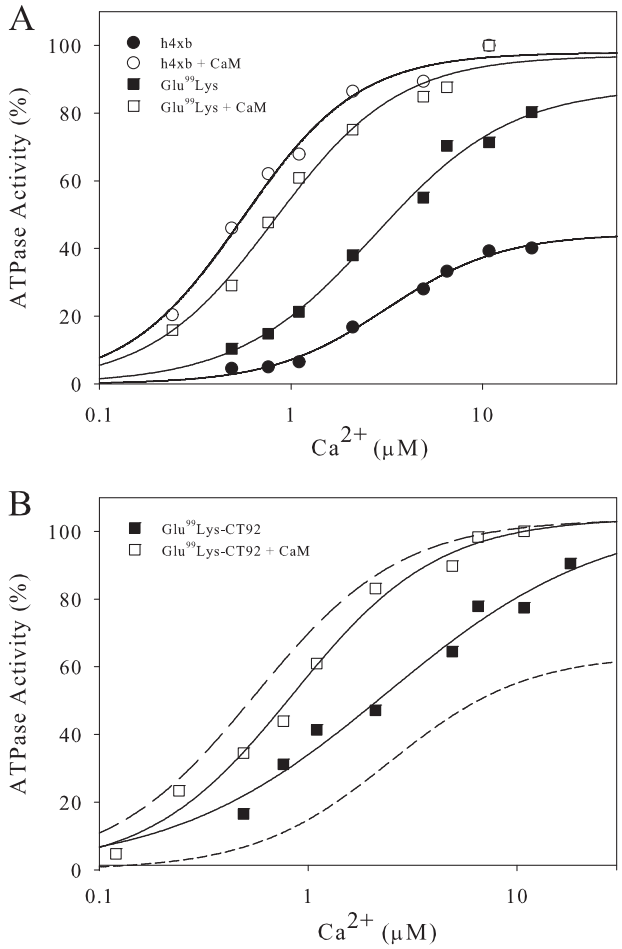

FIGURE 5. **Dependence of Ca^{2+}-ATPase activity of the E99K mutant and h4xb wild type (*A*) and the E99K-CT92 and CT92 (*B*) mutant enzymes on Ca^{2+} concentration.** The *dotted lines* in *B* represent the fit to the data of the CT92 mutant from Fig. 3 in the presence (*long dashes*) and in the absence (*short dashes*) of calmodulin. The Ca^{2+}-ATPase activity was assayed at variable free Ca^{2+} concentrations in the absence or presence of 200 nM calmodulin. The activities are expressed relative to the maximum activity of each enzyme measured at saturating Ca^{2+} in the presence of 200 nM calmodulin. The *lines* represent the best fit of the data given by the Hill equation.

tion of GFP in the E99K-CT92-GFP mutant resulted in a fully activated and calmodulin-insensitive enzyme (not shown).

The E99K and CT92-GFP Mutants Complemented the Yeast Strain K616—K616 cells lacking the Golgi PMR1 and vacuolar PMC1 Ca^{2+} ATPases and the regulatory subunit of calcineurin (CNB) do not proliferate when the medium contains low concentrations of Ca^{2+} (10 mM EGTA) (14, 20). As shown in Table 1, neither the K616 cells transformed with the empty expression vector pYX112 nor those expressing the wild type h4xb PMCA or mutant h4xb-GFP were able to grow in EGTA-containing medium. On the other hand, the expression of the fully active h4xb PMCA mutant CT120-GFP, lacking both the C and I autoinhibitory domains and containing the GFP fused at its C-terminal end, allowed K616 cells to grow in the medium containing low Ca^{2+}. The K616 cells expressing the CT92 mutant in which only the C-terminal autoinhibitory domain I was removed did not grow in the EGTA-containing medium. In contrast, successful complementation was obtained by expressing the fully activated/partially deregulated CT92-GFP, E99K, E99K-CT92, or E99K-CT92-GFP mutant enzymes.

TABLE 1

Phenotypic rescue of K616 yeast mutant by h4xb wild type and mutant PMCA pumps

K616 cells were transformed with empty vector or vector containing the DNA encoding for the wild type h4xb PMCA or the indicated mutants. The transformed cells were plated in medium containing either 10 mM $CaCl_2$ or 10 mM EGTA, and the growth (+) or its absence (−) was evaluated after 72 h.

Transfected K616	$CaCl_2$	EGTA
Empty vector	+	−
h4xb	+	−
CT120	+	+
CT92	+	−
h4xb-GFP	+	−
CT92-GFP	+	+
E99Q	+	−
E99K	+	+
E99K-CT92	+	+
E99K-CT92-GFP	+	+

TABLE 2

Comparison of the kinetic constants of h4xb wild type and mutant PMCA pumps

The kinetic constants were estimated by non-linear fitting of the Hill equation to the data of Ca^{2+}-ATPase as a function of Ca^{2+} concentrations of Figs.3–5. The maximal activity of each enzyme was determined at saturating concentrations of Ca^{2+} and calmodulin and used to calculate the percentage of V_{max} in the absence of calmodulin.

	$K_{0.5}$ Ca^{2+}		
	Without calmodulin	With calmodulin	V_{max} (% of the maximum) without calmodulin
	μM		%
h4xb	3.1 ± 0.1	0.6 ± 0.1	44 ± 2
h4xb-GFP	2.4 ± 0.1	0.6 ± 0.1	57 ± 2
CT92	2.4 ± 0.4	0.6 ± 0.1	63 ± 4
CT92-GFP	0.9 ± 0.2	0.7 ± 0.1	80 ± 1
E99K	2.7 ± 0.4	0.6 ± 0.1	98 ± 3
E99K-CT92	2.4 ± 0.1	0.8 ± 0.1	104 ± 14

DISCUSSION

A distinctive feature of type 2B Ca^{2+}-ATPases is that they contain calmodulin-responsive autoinhibitory domains. Loss of autoinhibition by the binding of Ca^{2+}-CaM allows a rapid 10-fold increase in their activity. In the present work, we constructed, expressed, and biochemically characterized different mutants of the h4xb PMCA with the aim to better understand the mechanism of autoinhibition. The kinetic constants of the wild type and mutant h4xb PMCA enzymes are summarized in Table 2. We found that the fusion of GFP to the C terminus of h4xb slightly increased the V_{max}. This increase is in the range of that obtained by the C-terminal truncation of 92 residues in the CT92 mutant, which involves the removal of subdomain I (9), indicating that the fusion of GFP to the C terminus of h4xb PMCA impairs the inhibition by domain I. Furthermore, the fusion of GFP to the C terminus of the CT92 mutant increased the V_{max} and the apparent affinity for Ca^{2+}. Altogether, these results indicate that the GFP moiety impairs the function of the domain that is immediately precedent, probably by sterically altering its docking with the autoinhibitory receptor site.

Previous studies have shown that the N-terminal region of the PMCA is involved in autoinhibition (15, 25). Here we found that mutation of residue Glu^{99} to Lys in the N-terminal portion of transmembrane helix M1 partially disinhibited the h4xb PMCA. In a previous random mutagenesis study of the autoinhibited plant ACA2, the E167K mutation, at the equivalent position of Glu^{99} of h4xb PMCA, was recovered in a screen for deregulated enzymes (14). In the ACA2, however, this mutation

increased both the apparent affinity for Ca^{2+} and the V_{max}, whereas in the h4xb PMCA, we found that it specifically increased the V_{max} without changing the apparent affinity for Ca^{2+}. This difference may either be due to the different experimental conditions, in particular the use of membrane fractions or purified enzymes, or reflect functional differences in the autoinhibition mechanism between animal and plant PMCAs. Because the increase in the V_{max} caused by the E99K mutation was more pronounced than that of the CT92 truncation, it would seem that the effects of the mutation are not limited to autoinhibitory domain I.

The phenotypic rescue of K616 yeast cells confirmed that h4xb mutants are still activated *in vivo*. This is important because it is well known that the autoinhibition of PMCA is highly dependent on the interaction with lipids and the detergent used during the purification of the protein (26). Neither the wild type h4xb pump nor the partially activated h4xb-GFP and CT92 mutants were able to rescue K616 cells from their inability to grow in low Ca^{2+} medium. In contrast, the expression of the E99K mutant allowed K616 cells to grow in a Ca^{2+}-depleted medium. Because the E99K mutant enzyme had a fully deregulated V_{max} at saturating Ca^{2+} concentrations, it seems that the increase in Ca^{2+} affinity is not a requisite for complementation. It should be considered, however, that *in vivo* the PMCA may be subjected to additional regulatory mechanisms that increase the apparent affinity for Ca^{2+} (*e.g.* the proteolysis of the C-terminal segment by caspase-3) (27).

Activation of h4xb by the E99K Mutation—The experiments reported here do not tell the precise mechanism by which the E99K mutation activates the h4xb PMCA, a knowledge that probably will have to await the determination of the x-ray structure of the autoinhibited form of the protein. However, it is interesting to consider that residue Glu^{99} is remarkably well conserved in all isoforms of human, insect, and worm PMCAs. This position also corresponds to Glu in the plant ACA pumps and to Glu or Gln in non-autoinhibited P2A-ATPases like sarcoendoplasmic Ca^{2+}-ATPase (SERCA) and Na^+/K^+-ATPase, respectively. Indeed, in SERCA, the residue corresponding to h4xb PMCA Glu^{99} is Glu^{55}, which, together with Glu^{51}, Glu^{58}, and Asp^{59}, forms a cluster of acidic residues at the N terminus of M1, which was originally speculated to be part of the Ca^{2+} binding site (28) and later to form a filter channel directing Ca^{2+} to its binding sites (29). The results of mutagenesis of these residues in SERCA to Leu, Arg, or Ala did not support that proposal because, with the exception of the Asp^{59} mutant, which has been shown to accelerate the Ca^{2+} dissociation, mutations of all other cluster residues have been reported to be wild type in all functional aspects (30, 31).

The crystal structures of SERCA allow the prediction that residue Glu^{99} of h4xb PMCA is in a conformationally sensitive location. Particularly interesting is the fact that, in the Ca_2E_1 form (Protein Data Bank code 1SU4), M1 is a straight helix, whereas the x-ray of SERCA in other conformational states shows M1 bent at Leu^{60} (see the structure of Ca_2E_1 with bound ADP and AlF^-, representing Ca_2E_1P-ADP, Protein Data Bank code 1T5T). This kink divides M1 in an N-terminal acidic segment, which adopts an orientation parallel to the membrane surface, and a C-terminal hydrophobic membrane-inserted segment. Hence, on the basis of the SERCA structure, the h4xb PMCA residue Glu^{99} would be part of the acidic platform formed by the N-terminal portion of M1. In agreement with the results of the mutagenesis studies of SERCA, we found that the replacement of Glu^{99} of the h4xb PMCA by Gln or Lys showed no detectable effect on the activity of the fully activated form of the enzyme. The presence of a Lys at position 99 resulted in a higher V_{max} only when the h4xb pump was autoinhibited, indicating that Glu^{99} is important for autoinhibition. It is tempting to think that, in P2B-ATPases, the acidic M1 is used for the regulation of the activity. The partial loss of autoinhibition by the E99K mutation reported here could be interpreted as a direct interaction of Glu^{99} with the autoinhibitory domain. Noticeably, the E99Q mutation had no detectable consequences on the autoinhibition of the pump, indicating that the deregulation was not due to the loss of a negatively charged residue but to the presence of a new positively charged one. This result may reflect the importance of the negative charge of Glu^{99} to anchor the C-terminal autoinhibitory sequences to the autoinhibitory receptor site. The occurrence of a positive charge in the E99K mutant may destabilize the interaction, as, we found, does the presence of GFP at the C terminus of h4xb PMCA. Alternatively, the E99K mutation may change the conformational flexibility of the M1 platform and indirectly change the autoinhibitory receptor site presumably formed by residues of the A and N domains.

The Calmodulin Binding Site of the C-terminal Region of h4xb—The amino acid sequence of the C-terminal region of some mammalian PMCA isoforms shows the presence of two CaMB sites homologous to those described for the ACA protein (11). The alternative splicing of mRNA in this region of the human PMCA generates the isoforms denominated a, b, d, and k. Whereas isoforms a, d, and k show the sequence of amino acids corresponding to both CaMB sites, the variant b apparently includes only one site at the same position. This agrees with previous studies showing that the binding of only one calmodulin to h4xb PMCA suffices for full activation (32, 33). Comparison of the sequence of the calmodulin-binding site of h4xb with that of the CaMBS1 and CaMBS2 of other isoforms shows that the h4xb calmodulin-binding site is a composite site formed by the 16 N-terminal residues of CaMBS1 and 12 C-terminal residues of CaMBS2. Previous studies have shown that peptides resembling the N-terminal half of the h4xb CaMBS bind calmodulin with 1000-fold lower affinity than the full-length 28-amino acid peptide corresponding to the full binding site, whereas a peptide with the sequence of the C-terminal half does not bind calmodulin (34). Thus, both portions of the CaMBS of h4xb corresponding to CaMBS1 and that corresponding to CaMBS2 would be required for calmodulin binding and autoinhibition.

The Interaction between the C-terminal Regulatory Region of the PMCA and the Catalytic Core of the Protein—In the autoinhibited state, the calmodulin-binding autoinhibitory sequences of the autoinhibited P2B-ATPases interact with the catalytic core. Recently, a structural model for ACA8 in its autoinhibited and Ca^{2+}-CaM-activated states has been proposed (11). According to this model, the N-terminal regulatory domain of ACA8 adopts the structure of a long helix that inserts vertically in a cleft of

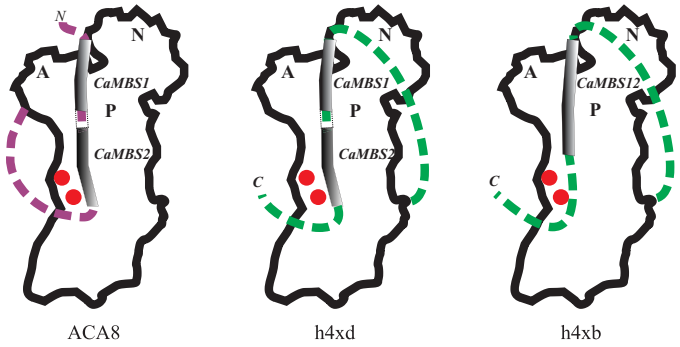

FIGURE 6. **Schematic representation of plant (ACA8) and human (h4xd and h4xb) P2B-Ca^{2+}-ATPases in their autoinhibited conformation.** The schematic models for the human PMCA isoforms h4xd and h4xb follow that proposed for ACA8 (11). The actuator (*A*), phosphorylation (*P*), and nucleotide (*N*) domains are indicated. The high affinity calmodulin-binding site, CaMBS1, the lower affinity site, CaMBS2, and the high affinity composite site of h4xb, CaMBS12, are shown. *Red dots*, approximate locations of residues Glu^{99} and Asp^{170} in the cytoplasmic helical portions of M1 and M2, respectively. Note that if the same residues would interact during autoinhibition in plant and human PMCAs, the autoinhibitory helix should adopt a *bottom* to *top* disposition in ACA8 and a *top* to *bottom* disposition in human PMCA, as shown.

acidic residues between the A and N/P domains, and the main autoinhibitory high affinity CaMBS1 interacts near the top of the A and N domains, whereas the second autoinhibitory CaMBS2 interacts deeper in the core of the protein with the linkers connecting the A domain with the transmembrane segments (Fig. 6). The results presented here and those of previous studies of the human PMCA are compatible with this model. However, in the case of h4xb, the autoinhibition by its CaMBS (domain C) at the A-N interface would decrease the V_{max} and the apparent Ca^{2+} affinity, whereas the interaction between the downstream C-terminal region (domain I) and the region of M1 near the membrane would provide additional autoinhibition by decreasing the V_{max}. Moreover, the C-terminal portion of the autoinhibitory segment would be flanked by Glu^{99} and Asp^{170} from the transmembrane segments M1 and M2, respectively. We have previously shown that Asp^{170} is a highly sensitive spot for autoinhibition and that even a conservative substitution by Asn increases the V_{max} and the apparent affinity for Ca^{2+} (35). Interestingly, although the basic features of the model may be shared by all autoinhibited Ca^{2+}-ATPases, there are probably also some differences. In fact, as already mentioned, both plant and animal PMCAs contain the CaM binding and autoinhibitory sequences at opposite ends, and thus their sequences are not symmetrical to the catalytic portion of the molecule (Fig. 6). Previous work by our laboratory and others has shown that the relative position of the autoinhibitory domain is not essential for autoinhibition (25, 36). However, relocating the calmodulin-binding autoinhibitory region of h4xb from the C terminus to the N terminus produces a mutant pump that has low apparent affinity for Ca^{2+} but a V_{max} higher than that of the autoinhibited pump, indicating that the autoinhibition function is somewhat perturbed (36). Thus, although the model proposed for ACA autoinhibition can be applied to the PMCA, the different disposition of the autoinhibitory sequences probably indicates that other compensatory structural features are necessary.

It is known that some PMCA isoforms and splice variants differ in their degree of autoinhibition and thus exhibit a distinct basal activity and sensitivity to activators (34, 37–39). A growing number of studies show the importance of a coordinated expression of different PMCA isoforms for normal cell function (40). Moreover, recent work has shown that PMCA4 is involved in specialized Ca^{2+}-handling processes (41, 42). Our results show that the presence of the negative charge provided by Glu^{99} is important for autoinhibition. Hence, affecting the charge at position 99 could be a possible strategy for therapeutic interventions seeking to increase the activity of the enzyme without changing its Ca^{2+} dependence.

REFERENCES

1. Di Leva, F. Domi, T., Fedrizzi, L., Lim, D., and Carafoli, E. (2008) The plasma membrane Ca^{2+}-ATPase of animal cells: structure, function and regulation. *Arch. Biochem. Biophys.* **476,** 65–74
2. Strehler, E. E., and Zacharias, D. A. (2001) Role of alternative splicing in generating isoform diversity among plasma membrane calcium pumps. *Phys. Rev.* **81,** 21–49
3. Palmgren, M. G., and Axelsen, K. B. (1998) Evolution of P-type ATPases. *Biochim. Biophys. Acta* **1365,** 37–45
4. Niggli, V., Adunyah, E. S., Penniston, J. T., and Carafoli, E. (1981) Purified (Ca^{2+}-Mg^{2+})-ATPase of the erythrocyte membrane. Reconstitution and effect of calmodulin and phospholipids. *J. Biol. Chem.* **256,** 395–401
5. Toyoshima, C., Nakasako, M., Nomura, H., and Ogawa, H. (2000) Crystal structure of the calcium pump of sarcoplasmic reticulum at 2.6 Å resolution. *Nature* **405,** 647–655
6. Palmgren, M. G., and Nissen, P. (2011) P-Type ATPases. *Annu. Rev. Biophys.* **40,** 243–266
7. Enyedi, A., Verma, A. K., Filoteo, A. G., and Penniston, J. T. (1996) Protein kinase C activates the plasma membrane Ca^{2+} pump isoform 4b by phosphorylation of an inhibitory region downstream of the calmodulin-binding domain. *J. Biol. Chem.* **271,** 32461–32467
8. Kim, E., DeMarco, S. J., Marfatia, S. M., Chishti, A. H., Sheng, M., and Strehler, E. E. (1998) Plasma membrane Ca^{2+}-ATPase isoform 4b binds to membrane-associated guanylate kinase (MAGUK) proteins via their PDZ (PSD-95/Dlg/ZO-1) domains. *J. Biol. Chem.* **273,** 1591–1595
9. Verma, A. K., Enyedi, A., Filoteo, A. G., and Penniston, J. T. (1994) Regulatory region of plasma membrane Ca^{2+} pump. 28 residues suffice to bind calmodulin but more are needed for full auto-inhibition of the activity. *J. Biol. Chem.* **269,** 1687–1691
10. Enyedi, A., Verma, A. K., Filoteo, A. G., and Penniston, J. T. (1993) A highly active 120-kDa truncated mutant of the plasma membrane Ca^{2+} pump. *J. Biol. Chem.* **268,** 10621–10626
11. Tidow, H., Poulsen, L. R., Andreeva, A., Knudsen, M., Hein, K. L., Wiuf, C., Palmgren, M. G., and Nissen, P. (2012) A bimodular mechanism of calcium control in eukaryotes. *Nature* **491,** 468–472
12. Vorherr, T., Quadroni, M., Krebs, J., and Carafoli, E. (1992) Photoaffinity labeling study of the interaction of calmodulin with the plasma membrane Ca^{2+} pump. *Biochemistry* **31,** 8245–8251
13. Falchetto, R., Vorherr, T., and Carafoli, E. (1992) The calmodulin-binding site of the plasma membrane Ca^{2+} pump interacts with the transduction domain of the enzyme. *Protein Sci.* **1,** 1613–1621
14. Curran, A. C., Hwang, I., Corbin, J., Martinez, S., Rayle, D., Sze, H., and Harper, J. F. (2000) Autoinhibition of a calmodulin-dependent calcium pump involves a structure in the stalk that connects the transmembrane domain to the ATPase catalytic domain. *J. Biol. Chem.* **275,** 30301–30308
15. Corradi, G. R., and Adamo, H. P. (2007) Intramolecular fluorescence resonance energy transfer between fused autofluorescent proteins reveals rearrangements of the N- and C-terminal segments of the plasma membrane Ca^{2+} pump involved in the activation. *J. Biol. Chem.* **282,** 35440–35448
16. Sarkar, G., and Sommer, S. S. (1990) The "megaprimer" method of site-directed mutagenesis. *BioTechniques* **8,** 404–407
17. Corradi, G. R., de Tezanos Pinto, F., Mazzitelli, L. R., and Adamo, H. P. (2012) Shadows of an absent partner: ATP hydrolysis and phosphoenzyme turnover of the Spf1 (sensitivity to *Pichia farinosa* killer toxin) P5-ATPase. *J. Biol. Chem.* **287,** 30477–30484

18. Bauer, A., and Kolling, R. (1996) The SAC3 gene encodes a nuclear protein required for normal progression of mitosis. *Yeast* **12,** 965–975
19. Elble, R. (1992) A simple and efficient procedure for transformation of yeasts. *Biotechnology* **13,** 18–20
20. Cunningham, K. W., and Fink, G. R. (1994) Calcineurin-dependent growth control in *Saccharomyces cerevisiae* mutants lacking PMC1, a homolog of plasma membrane Ca^{2+} ATPases. *J. Cell Biol.* **124,** 351–363
21. Richards, D. E., Rega, A. F., and Garrahan, P. J. (1978) Two classes of site for ATP in the Ca^{2+}-ATPase from human red cell membranes. *Biochim. Biophys. Acta* **511,** 194–201
22. Adamo, H. P., Caride, A. J., and Penniston, J. T. (1992) Use of expression mutants and monoclonal antibodies to map the erythrocyte Ca^{2+} pump. *J. Biol. Chem.* **267,** 14244–14249
23. Laemmli, U. K. (1970) Cleavage of structural proteins during the assembly of the head of bacteriophage T4. *Nature* **227,** 680–685
24. Bradford, M. (1976) A rapid and sensitive method for the quantitation of microgram quantities of protein utilizing the principle of protein-dye binding. *Anal. Biochem.* **72,** 248–254
25. Bonza, M. C., and Luoni, L. (2010) Plant and animal type 2B Ca^{2+}-ATPases: evidence for a common auto-inhibitory mechanism. *FEBS Lett.* **584,** 4783–4788
26. Cura, C. I., Corradi, G. R., Rinaldi, D. E., and Adamo, H. P. (2008) High sensibility to reactivation by acidic lipids of the recombinant human plasma membrane Ca^{2+}-ATPase isoform 4xb purified from *Saccharomyces cerevisiae*. *Biochim. Biophys. Acta* **1778,** 2757–2764
27. Pászty, K., Antalffy, G., Penheiter, A. R., Homolya, L., Padányi, R., Iliás, A., Filoteo, A. G., Penniston, J. T., and Enyedi, A. (2005) The caspase-3 cleavage product of the plasma membrane Ca^{2+}-ATPase 4b is activated and appropriately targeted. *Biochem. J.* **391,** 687–692
28. MacLennan, D. H., Brandl, C. J., Korczak, B., and Green, N. M. (1985) Amino-acid sequence of a Ca^{2+}- Mg^{2+}-dependent ATPase from rabbit muscle sarcoplasmic reticulum, deduced from its complementary DNA sequence. *Nature* **316,** 696–700
29. Lee, A. G., and East, J. M. (2001) What the structure of a calcium pump tells us about its mechanism. *Biochem. J.* **356,** 665–683
30. Einholm, A. P., Andersen, J. P., and Vilsen, B. (2007) Roles of transmembrane segment M1 of Na^+,K^+-ATPase and Ca^{2+}-ATPase, the gatekeeper and the pivot. *J. Bioenerg. Biomembr.* **39,** 357–366
31. Daiho, T., Yamasaki, K., Danko, S., and Suzuki, H. (2007) Critical role of Glu^{40}-Ser^{48} loop linking actuator domain and first transmembrane helix of Ca^{2+}-ATPase in Ca^{2+} deocclusion and release from ADP-insensitive phosphoenzyme. *J. Biol. Chem.* **282,** 34429–34447
32. James, P., Maeda, M., Fischer, R., Verma, A. K., Krebs, J., Penniston, J. T., and Carafoli, E. (1988) Identification and primary structure of a calmodulin binding domain of the Ca^{2+} pump of human erythrocytes. *J. Biol. Chem.* **263,** 2905–2910
33. Filoteo, A. G., Enyedi, A., and Penniston, J. T. (1992) The lipid-binding peptide from the plasma membrane Ca^{2+} pump binds calmodulin, and the primary calmodulin-binding domain interacts with lipid. *J. Biol. Chem.* **267,** 11800–11805
34. Enyedi, A., Filoteo, A. G., Gardos, G., and Penniston, J. T. (1991) Calmodulin-binding domains from isozymes of the plasma membrane Ca^{2+} pump have different regulatory properties. *J. Biol. Chem.* **266,** 8952–8956
35. Bredeston, L. M., and Adamo, H. P. (2004) Loss of autoinhibition of the plasma membrane Ca^{2+} pump by substitution of aspartic 170 by asparagine. Activation of plasma membrane calcium ATPase 4 without disruption of the interaction between the catalytic core and the C-terminal regulatory domain. *J. Biol. Chem.* **279,** 41619–41625
36. Adamo, H. P., and Grimaldi, M. E. (1998) Functional consequences of relocating the C-terminal calmodulin-binding autoinhibitory domains of the plasma membrane Ca^{2+} pump near the N-terminus. *Biochem. J.* **331,** 763–766
37. Enyedi, A., Verma, A. K., Heim, R., Adamo, H. P., Filoteo, A. G., Strehler, E. E., and Penniston, J. T. (1994) The Ca^{2+} affinity of the plasma membrane Ca^{2+} pump is controlled by alternative splicing. *J. Biol. Chem.* **269,** 41–43
38. Caride, A. J., Penheiter, A. R., Filoteo, A. G., Bajzer, Z., Enyedi, A., and Penniston, J. T. (2001) The plasma membrane calcium pump display memory of past calcium spikes. Differences between isoforms 2b and 4b. *J. Biol. Chem.* **276,** 39797–39804
39. Kozel, P. J., Friedman, R. A., Erway, L. C., Yamoah, E. N., Liu, L. H., Riddle, T., Duffy, J. J, Doetschman, T., Miller, M. L., Cardell, E. L., and Shull, G. E. (1998) Balance and hearing deficits in mice with a null mutation in the gene encoding plasma membrane Ca^{2+}-ATPase isoform 2. *J. Biol. Chem.* **273,** 18693–18696
40. Strehler, E. E., Caride, A. J., Filoteo, A. G., Xiong, Y., Penniston, J. T., and Enyedi, A. (2007) Plasma membrane Ca^{2+} ATPases as dynamic regulators of cellular calcium handling. *Ann. N. Y. Acad. Sci.* **1099,** 226–236
41. Curry, M. C., Luk, N. A., Kenny, P. A., Roberts-Thomson, S. J., and Monteith, G. R. (2012) Distinct regulation of cytoplasmic calcium signals and cell death pathways by different plasma membrane calcium ATPase isoforms in MDA-MB-231 breast cancer cells. *J. Biol. Chem.* **287,** 28598–28608
42. Okunade, G. W., Miller, M. L., Pyne, G. J., Sutliff, R. L., O'Connor, K. T., Neumann, J. C, Andringa, A., Miller, D. A., Prasad, V., Doetschman, T., Paul, R. J., and Shull, G. E. (2004) targeted ablation of plasma membrane Ca^{2+}-ATPase (PMCA) 1 and 4 indicates a major housekeeping function for PMCA 1 and a critical role in hyperactivated sperm motility and male fertility for PMCA4. *J. Biol. Chem.* **279,** 33742–33750

Membrane Biology:

Hyperactivation of the Human Plasma Membrane Ca^{2+} Pump PMCA h4xb by Mutation of Glu^{99} to Lys

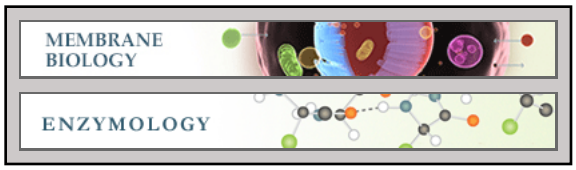

Luciana R. Mazzitelli and Hugo P. Adamo

J. Biol. Chem. 2014, 289:10761-10768.
doi: 10.1074/jbc.M113.535583 originally published online February 28, 2014